ORGANISATION EUROPEENNE POUR LA RECHERCHE NUCLEAIRE

CERN EUROPEAN ORGANIZATION FOR NUCLEAR RESEARCH

Radiation and induced activation at high luminosity

The effects on radiation levels and background rates of an increase of the luminosity at the LHC from 10^{34} cm^{-2} s^{-1} to 10^{35} cm^{-2} s^{-1} have been studied. Induced activation will be a large problem for ATLAS already at nominal luminosity and at higher luminosities the maintenance of the ATLAS detectors could be severely restricted. A change of material in the beampipe from stainless steel to beryllium would reduce the activation of the beampipe by three orders of magnitude. A change to a beryllium beampipe would also significantly lower the background rates in the muon spectrometer. Several new shielding scenarios have been simulated but there is no simple improvement of the shielding that would give a large reduction in muon background rates. Even drastic and very costly changes to the shielding will not reduce the background rates by more than a factor of three.

Prepared	Checked by:	Approved by:
Vincent Hedberg ***Mike Shupe***		

Distribution List

ATL-TECH-2004-002
22 November 2004

1 Introduction

The ATLAS collaboration is at present studying the possibility of running the detector at a luminosity much higher than the present design luminosity of 10^{34} $cm^{-2}s^{-1}$. This would have serious implications for many of the detector systems. This note deals with issues related to the increased radiation levels, both during running and shutdown periods. The increased radiation levels due to a higher interaction rate would lead to new radioprotection problems (particularly in the electronics cavern), to increased radiation damage to detectors and electronics and to an increased rate of background in the muon spectrometer. The level of induced radioactivity would also rise proportionally to the increase in the luminosity and this would make access and maintenance more difficult. The purpose of this note is to describe some of these problems and to discuss how the problems can be reduced by introducing changes of the shielding or other parts of the experiment. The engineering and economical difficulties that the various changes would lead to will in general not be addressed.

2 Radioprotection during LHC running

The USA15 cavern next to the ATLAS experimental cavern is going to house most of the electronics in the experiment. This is a large cavern that is 20 m wide and 62 m long with electronic racks on two floors (see Figure 1). It is necessary that people can visit and work for long periods in this cavern, even during high luminosity running, and it has been a design requirement that the USA15 cavern can be classified as a simple controlled area. The ambient dose equivalent limit for such an area is at present 25 μSv/h [1]. This limit was set based on a yearly maximum dose of 50 mSv (the present yearly dose is 20 mSv) and it is expected to be lowered in the future, probably to something like 10 μSv/h.

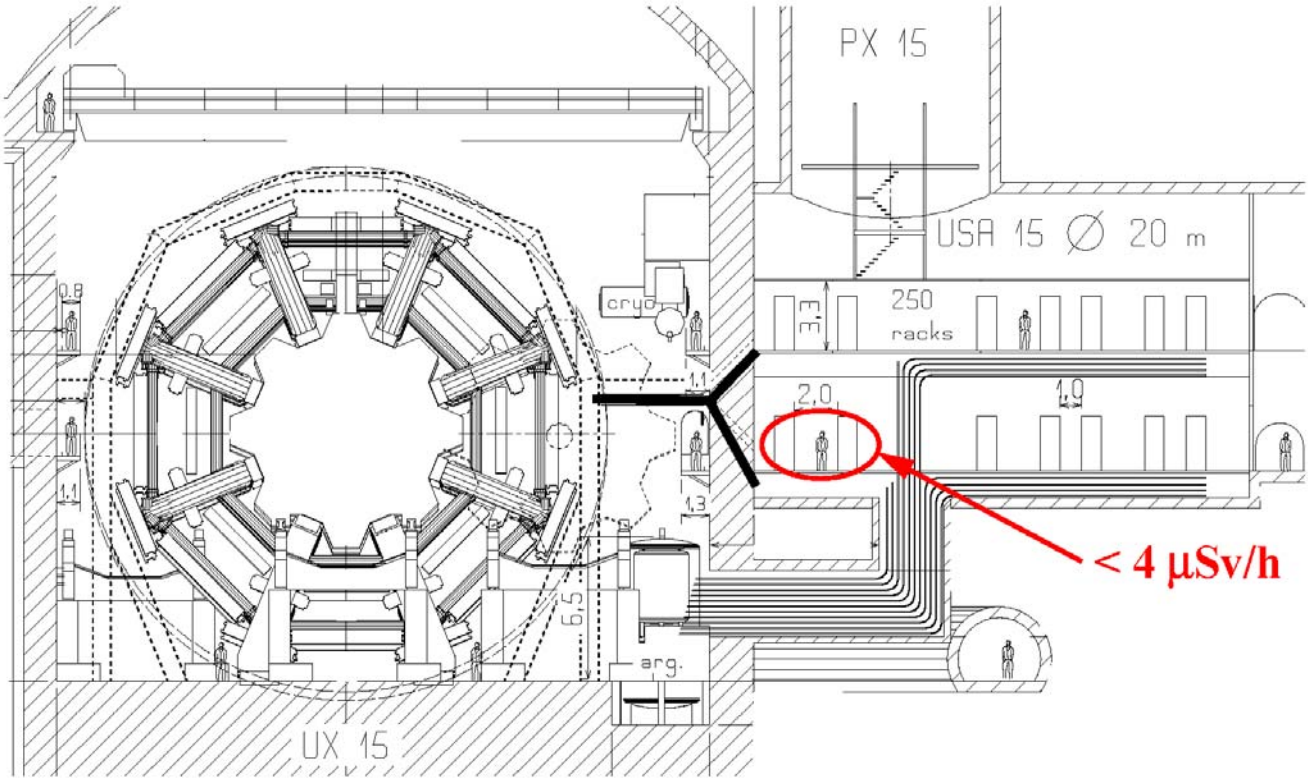

Figure 1. Cross section of the ATLAS experimental hall UX15 and the electronics cavern USA15.

A recent study by I. Dawson and V. Hedberg [2] predicts that the radiation levels in USA15 could reach 4 μSv/h when the luminosity is 10^{34} $cm^{-2}s^{-1}$. Since the uncertainty in these types of calculations is at best a factor 2-3 it could be that the radiation levels already at 10^{34} $cm^{-2}s^{-1}$ will be too high for a simple controlled area. If the luminosity is increased to 10^{35} $cm^{-2}s^{-1}$ it is almost certain that USA15 could not anymore be classified as a simple controlled area. This would not mean that the access by ATLAS members to USA15 would be completely prohibited but access would have to be much more limited.

Dawson and Hedberg recommend in their note that the 2 m thick concrete wall between UX15 and USA15 is strengthen by 20 cm of polyethylene on the USA15 side of the wall. The polyethylene would moderate the neutrons and the lower neutron energies would result in a factor of two reduction of the effective dose in USA15. It is, however, doubtful that this would be enough if the luminosity were increased to 10^{35} $cm^{-2}s^{-1}$.

Another area of concern is the ATLAS surface building (SX1) that is classified as a supervised area in which the effective dose rate should not exceed 2.5 μSv/h. The access shafts PX14 and PX16 will be covered by 100 cm thick concrete plugs during LHC running. The present prediction is that the dose rate above the largest shaft (PX14) will be 9 μSv/h at 10^{35} $cm^{-2}s^{-1}$, i.e., significantly larger than what is allowed for a supervised area. As long as the plug region in SX1 is properly fenced in, it might, however, not be a problem.

3 Induced activation

M. Morev and co-workers at the Moscow Engineering Physics Institute have made detailed calculations of the induced activation in ATLAS. A web-site [3] has been set-up with detailed information about all the ATLAS activation calculations and here only a few examples of the results will be discussed.

The method [4,5] that was used by the MEPhI group to calculate the activity was based on the standard activation formula that relates particle cross-sections and flux with the activity. Particle flux maps were produced by M. Shupe using the PHOJET [6] and GCALOR programs [7] under the assumptions of 7x7 TeV collisions and a luminosity of 10^{34} cm^{-2} s^{-1} giving a p-p interaction rate of $8x10^{8}$ s^{-1}. The flux maps were then used as inputs in the calculations of the activity. The calculations were made separately for (n,γ) capture of low-energy thermal neutrons and high-energy hadrons. In the latter case the lack of knowledge of the cross sections above 20 MeV for all possible types of interactions made it necessary to make the assumption that the cross section of all incident hadrons would be the same as that of protons [8]. The codes DOT-III [9] and MCNP [10] were used to calculate self-absorption and photon transport. Only gamma radiation was calculated. An LHC year was assumed to consist of 120 days of continuing running with a 245-day stop.

Figures 2 and 3 shows the expected dose rate in the region between the endcap toroid and the TX1S shielding with the TAS collimator. One can see that with the VJ beampipe in place, the predicted dose rate will exceed several mSv/h at 10^{35} $cm^{-2}s^{-1}$ if the distance to the beampipe is less than 1 m. Close to the VT beampipe and the TAS collimator the dose rate could exceed 10 mSv/h and work in this region is almost impossible. The dose rate as a function of cooling-off time is given for one point close to the TAS. In order to lower the dose rate by an order of magnitude, the cooling-off time has to be longer than 100 days, i.e., most of the winter shutdown would have to be used to wait for the equipment to cool down.

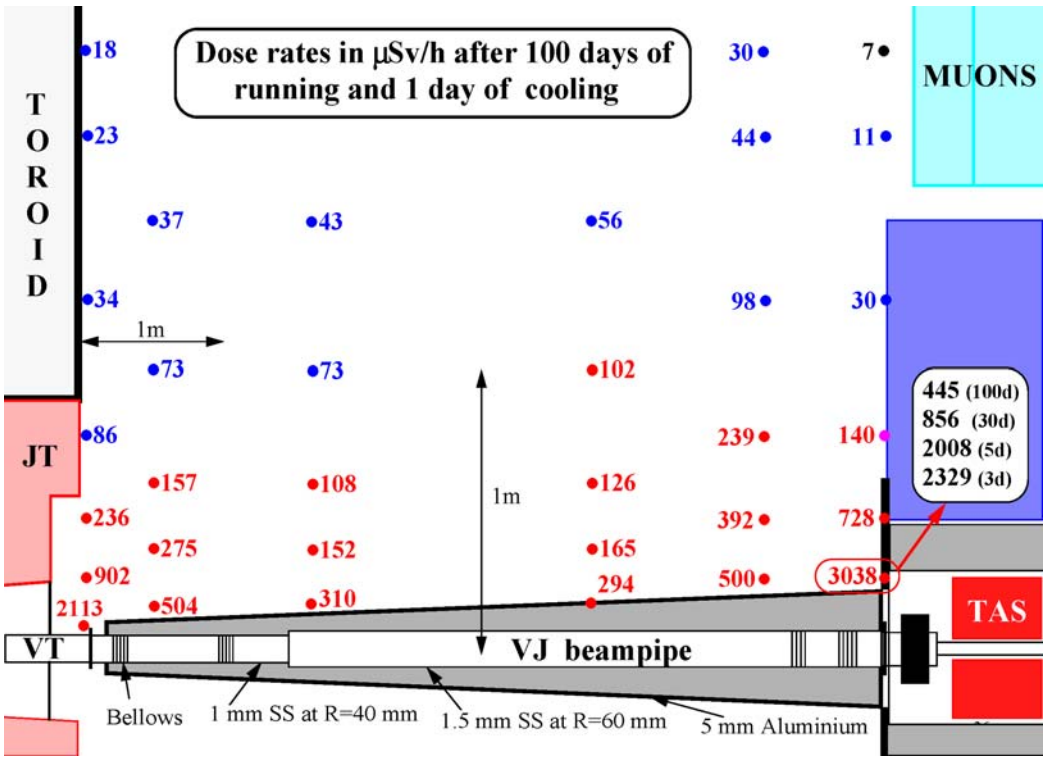

Figure 2. Dose rates in the region between the endcap toroid and the TX1S shielding after 100 days of running at 10^{34} cm^{-2}s^{-1} and one day of cooling off. The dose rates after other cooling-off times are given for one point. The calculation was done by Morev et al. [11].

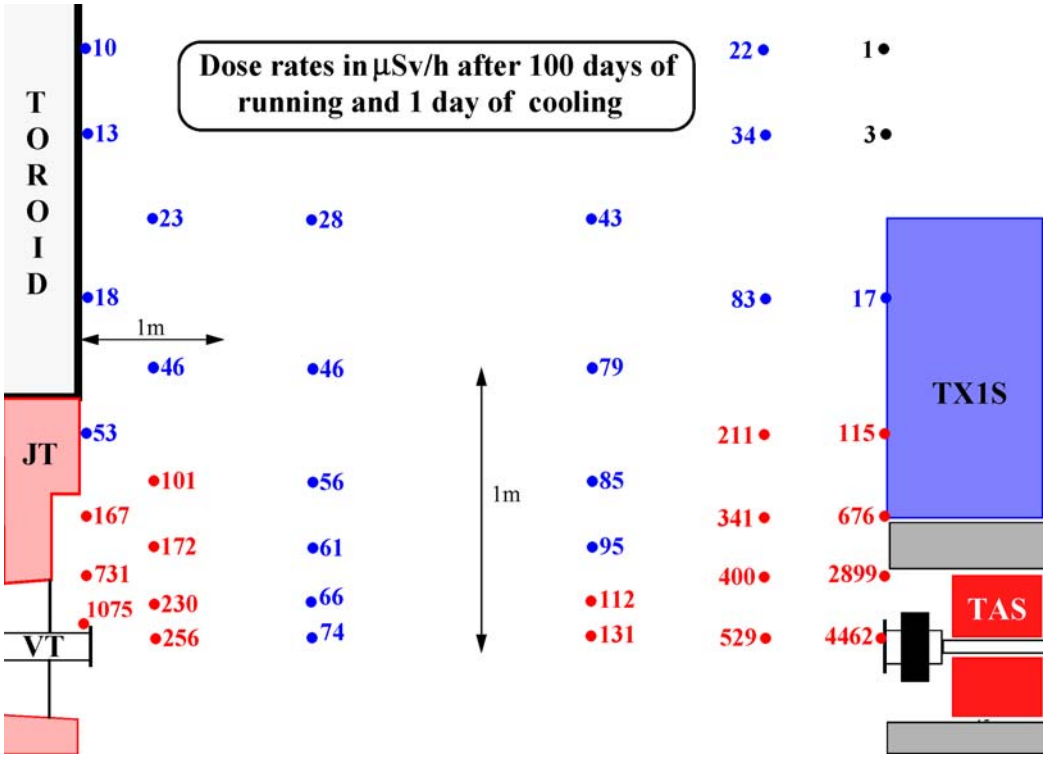

Figure 3. Dose rates in the region between the endcap toroid and the TX1S shielding after the beampipe has been removed and after 100 days of running at 10^{34} cm^{-2}s^{-1} and one day of cooling off. The calculation was done by Morev et al. [11].

Figures 3 shows that the dose rates are very large also after the VJ beampipe has been removed. This is mostly due to the remaining vacuum equipment with the VT beampipe on one side and the TAS collimator on the other.

Another example of a region with a very hot beampipe is the region in front of the inner detector that is depicted in Figure 4. With a stainless steel beampipe and a luminosity of 10^{35} $cm^{-2}s^{-1}$ the contact dose rate could reach 60 mSv/h in the region activated by the particles from the forward calorimeter. At these levels it is doubtful that the VA beampipe could be removed and that the inner detector could be reached for maintenance. The high dose rates already at 10^{34} $cm^{-2}s^{-1}$ has led to the suggestion that the beampipe in ATLAS should be made of aluminium instead of stainless steel. Figure 4 suggests that an aluminium beampipe could reduce the dose rates by a factor of 10 but the reduction factor depends strongly on the running and cooling-off times as can be seen in Figure 5. When the running time is long the advantage of an aluminium beampipe is diminished. The reason for this is the Na-22 isotope that is produced in aluminium during activation. This isotope has a half-life of 2.6 years and it therefore takes a very long time for it to reach an equilibrium state were as much Na-22 is produced as is decaying in a certain time window. When this equilibrium state has been reached the reduction factor obtained by going to an aluminium beampipe is less than 10.

A more efficient but also more costly solution to problem of the very radioactive beampipe would be to make it out of beryllium. Figure 6 shows the dose rate from the inner detector beampipe which is already at present going to be made out of beryllium. For both long and short running times the expected dose rates are only a few μSv/h and this is thousand times lower than what one would expect from a stainless steel beampipe and hundreds of times less than what would be expected from an aluminium beampipe (this can be seen at the end of the VI beampipe in Figure 6 since it is made of aluminium). The reason for the low activity from beryllium is that with this low-Z material it is only possible to produce Be-7 as a gamma-emitting isotope.

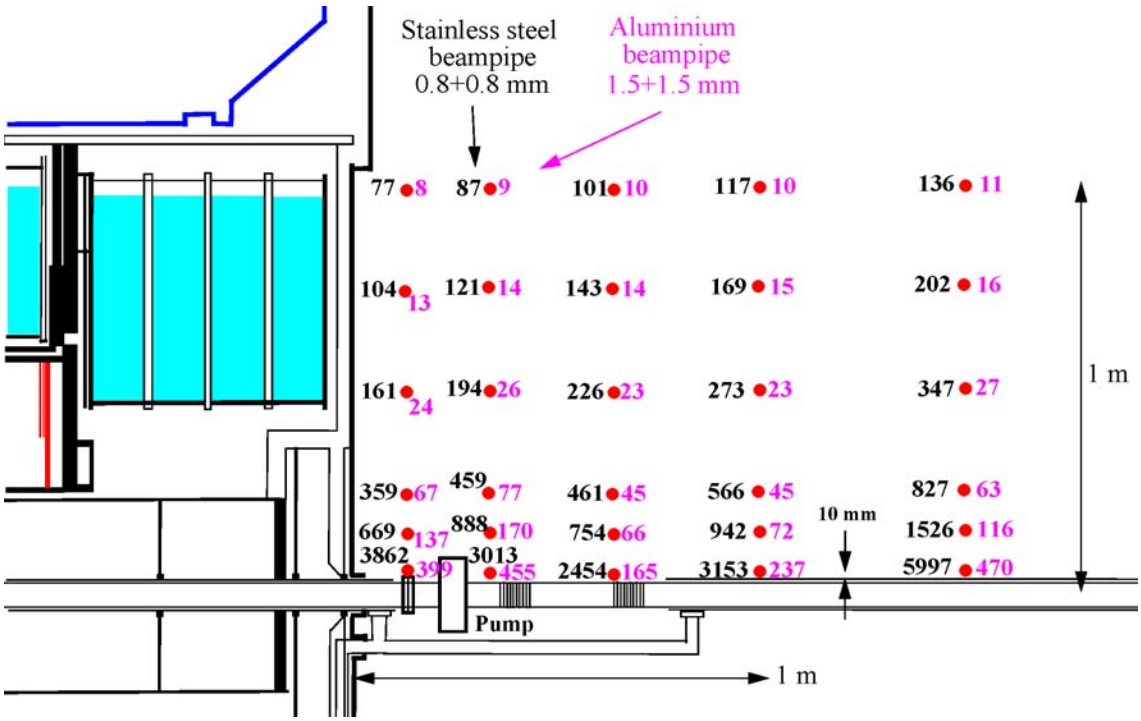

Figure 4. Dose rates (in μSv/h) in front of the inner detector after 10 years of running at 10^{34} $cm^{-2}s^{-1}$ and five days of cooling off. Dose rates are given for both a stainless steel and an aluminium beampipe. The calculation was done by Morev et al. [12].

Cooling time	Running time			
	5000d	1000d	100d	30d
1 d:	9	13	23	23
5 d:	9	15	76	181
7 d:	8	14	68	164
30 d:	4	7	22	39

Figure 5. The ratio of the dose rate from a steel and an aluminium beampipe with the same thickness for different running and cooling-off times.

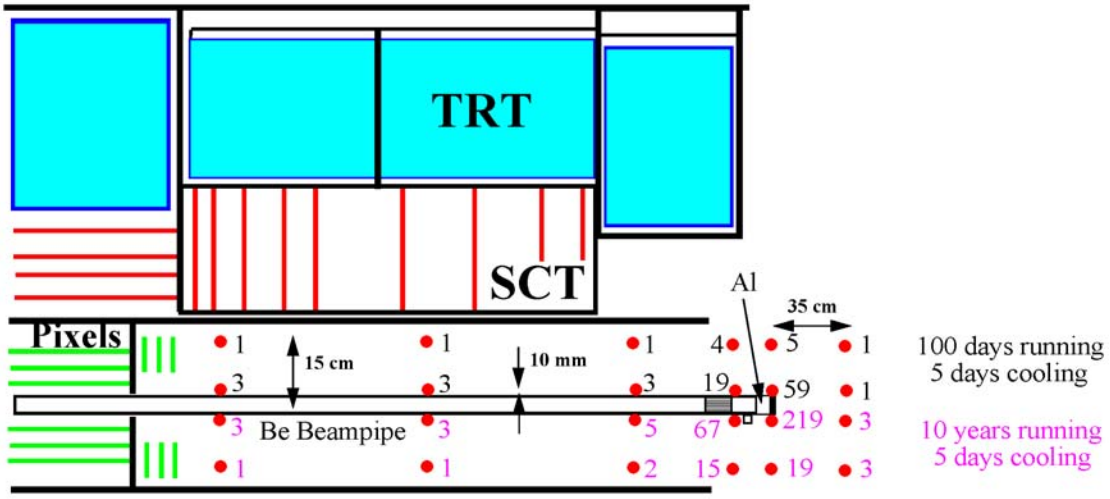

Figure 6. Dose rates (in μSv/h) from the beryllium beampipe in the inner detector after both 100 days and 10 years of running at 10^{34} $cm^{-2}s^{-1}$ and five days of cooling off. The calculation was done by Morev et al. [13].

4 Background in the muon spectrometer

The ATLAS Radiation Task Force has recently made new estimations of the single muon counting rates and the penetrating particle rates [14]. M. Bosman has folded the energy spectra calculated by GCALOR and FLUKA [15] with the efficiencies of the muon chambers to various types of particle fluxes as calculated by S. Baranov using GEANT3. The average efficiencies for different particles in different chambers have then been used to estimate the single counting rate for RPC, MDT and CSC detectors in the muon spectrometer. The result is given in Figure 7 together with predicted rates taken from the Muon Technical Design Report [16]. The new estimations of rates are the same or lower as those of the Muon TDR, with the exception of the Large Muon Wheel where the new rates are up to twice as large as those in the TDR. It is, however, not enough to estimate the rates in the muon spectrometer since it is also necessary to know the maximum rate at which the chambers can operate. There are no limits on the absolute rates in the TDR but the following statement is made: "*The ATLAS muon instrumentation is designed to operate at a nominal luminosity of* 10^{34} $cm^{-2}s^{-1}$*, allowing for a safety factor of five on the background rates*". This indicates that the MDTs should be able to cope with single counting rates of 500 Hz/cm^2 (at least in the small wheel).

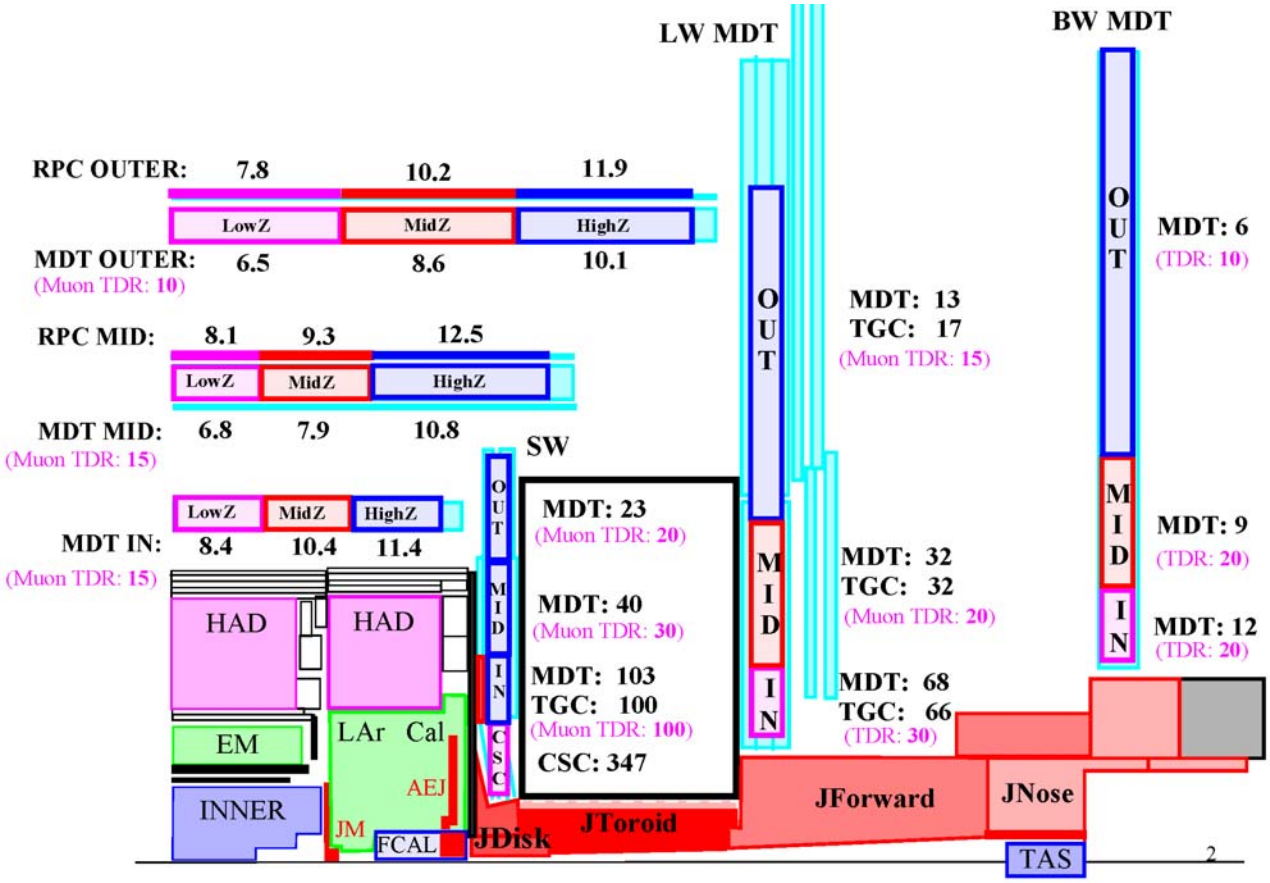

Figure 7. Muon chamber single counting rates in Hz/cm^2 at 10^{34} cm^{-2}s^{-1}. Predicted rates that were presented in the Muon Technical Design report [16] are also given. The rates were calculated by M.Bosman from efficiencies calculated by S. Baranov and particle rates calculated by M. Shupe and I.Dawson [15].

If one assumes that the luminosity will go up by one order of magnitude from the design luminosity, one could in principle compensate for this by simply making the rapidity coverage of the muon spectrometer smaller. Figure 8 and 9 shows the photon and neutron flux in one quadrant of the ATLAS experiment. The calculation was made for the September 2004 shielding baseline in GCALOR. Figure 8 shows that one has to go out to about 25° (η=1.5) if one wants to reduce the photon flux at the edge of the present muon spectrometer by an order of magnitude. Figure 9 shows that the neutron flux at 25° in the small wheel is also about ten times lower than at the outer edge of the present η-acceptance. In the large wheel the neutron flux is almost independent of the angle due to the effective neutron moderator situated on the outside of the endcap toroid wall.

The beampipe

It has been seen in previous studies by the Radiation Task Force that the beampipe is one of the major sources of background in the muon spectrometer. Figure 10 shows the five different beampipe sections in ATLAS and their dimensions. The very narrow bore in the forward calorimeter, and the requirement that the endcap calorimeter can be moved back when the beampipe is in place, has limited the outer radius of a large part of the beampipe to 30 mm.

The first question to ask is how much of the background that is produced in the beampipe. Figure 11 gives the answer to this question. The figure gives the ratio of the rates with and without a beampipe in one quadrant of ATLAS and for seven different scoring regions. The rates that are used in the figure are the single muon rates and the penetrating particle rates that are defined in the following way:

Single counting rate = 0.0005n + 0.0117γ + (μ + p + π + 0.25e)/2

Penetrating particle rate = 0.0117γ + (μ + p + π + 0.25e)/2

where n, γ, μ, p, π and e are the fluxes of neutrons, photons, muons, protons, pions and electrons respectively.

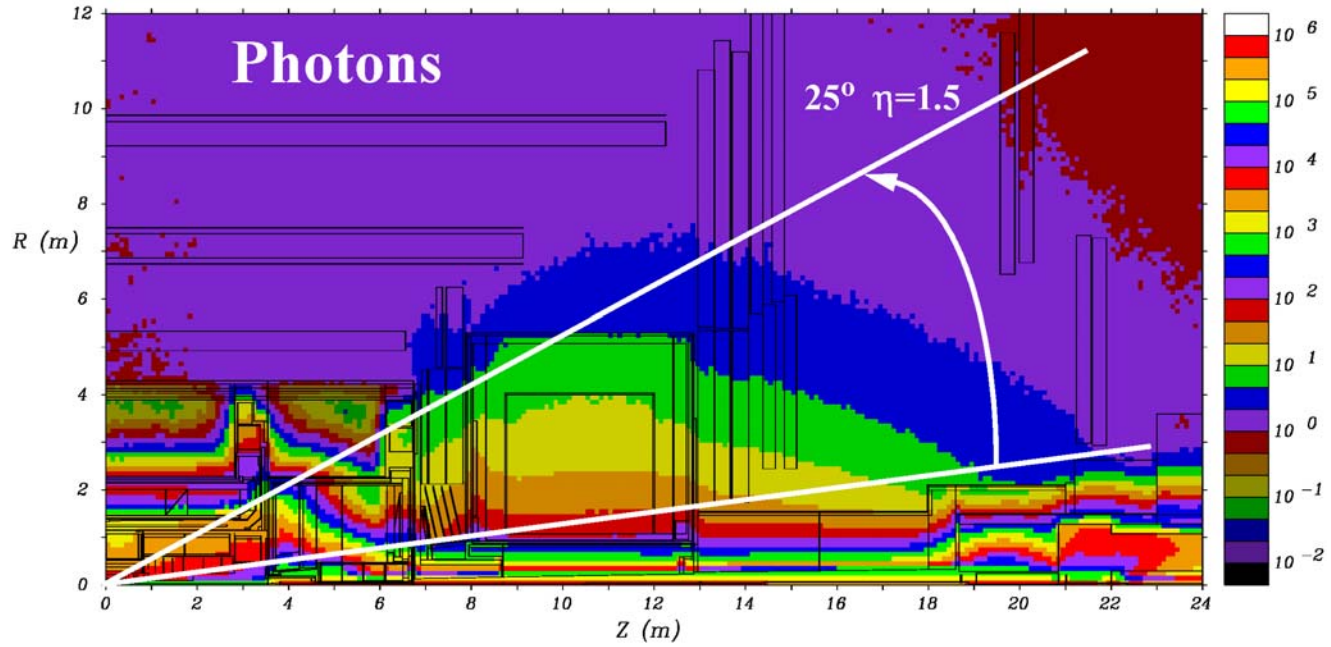

Figure 8. The photon flux in kHz/cm^2 at 10^{34} cm^{-2}s^{-1} in one quadrant of the ATLAS experiment. The white lines indicate how the acceptance of the muon spectrometer would have to be changed in order to reduce the maximum photon flux by a factor of ten in the small and big wheel.

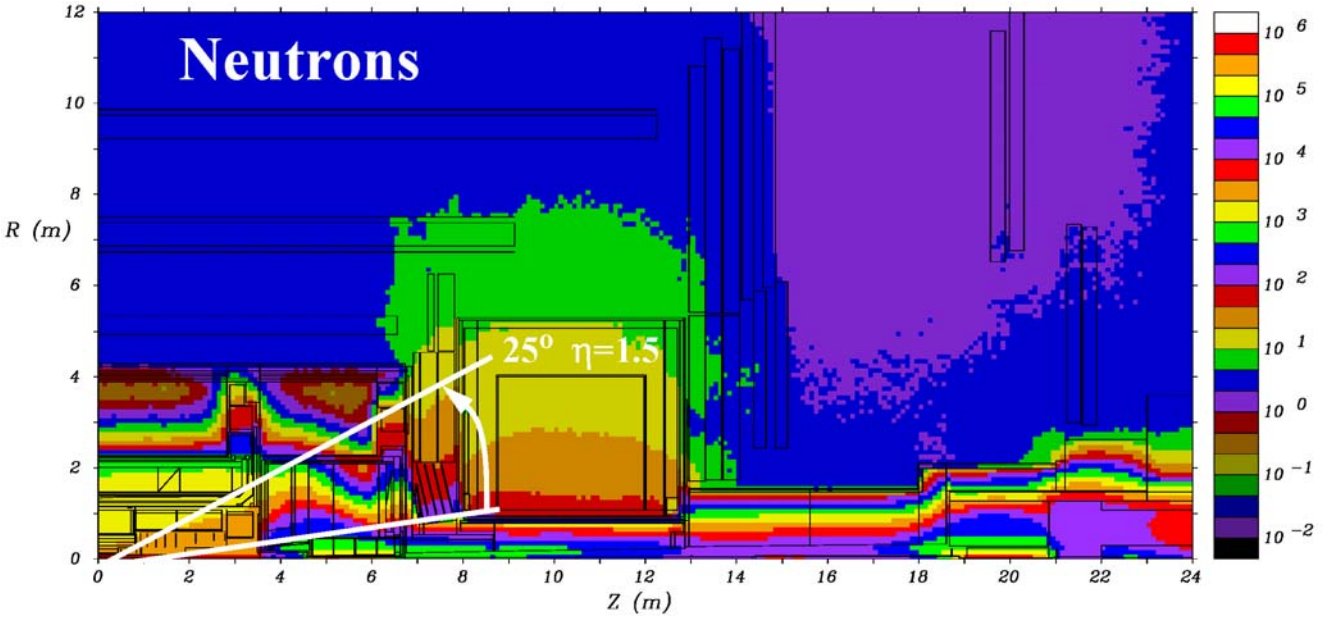

Figure 9. The neutron flux in kHz/cm^2 at 10^{34} cm^{-2}s^{-1} in one quadrant of the ATLAS experiment. The white lines indicate how the acceptance of the muon spectrometer would have to be changed in order to reduce the maximum neutron flux by a factor of ten in the small wheel.

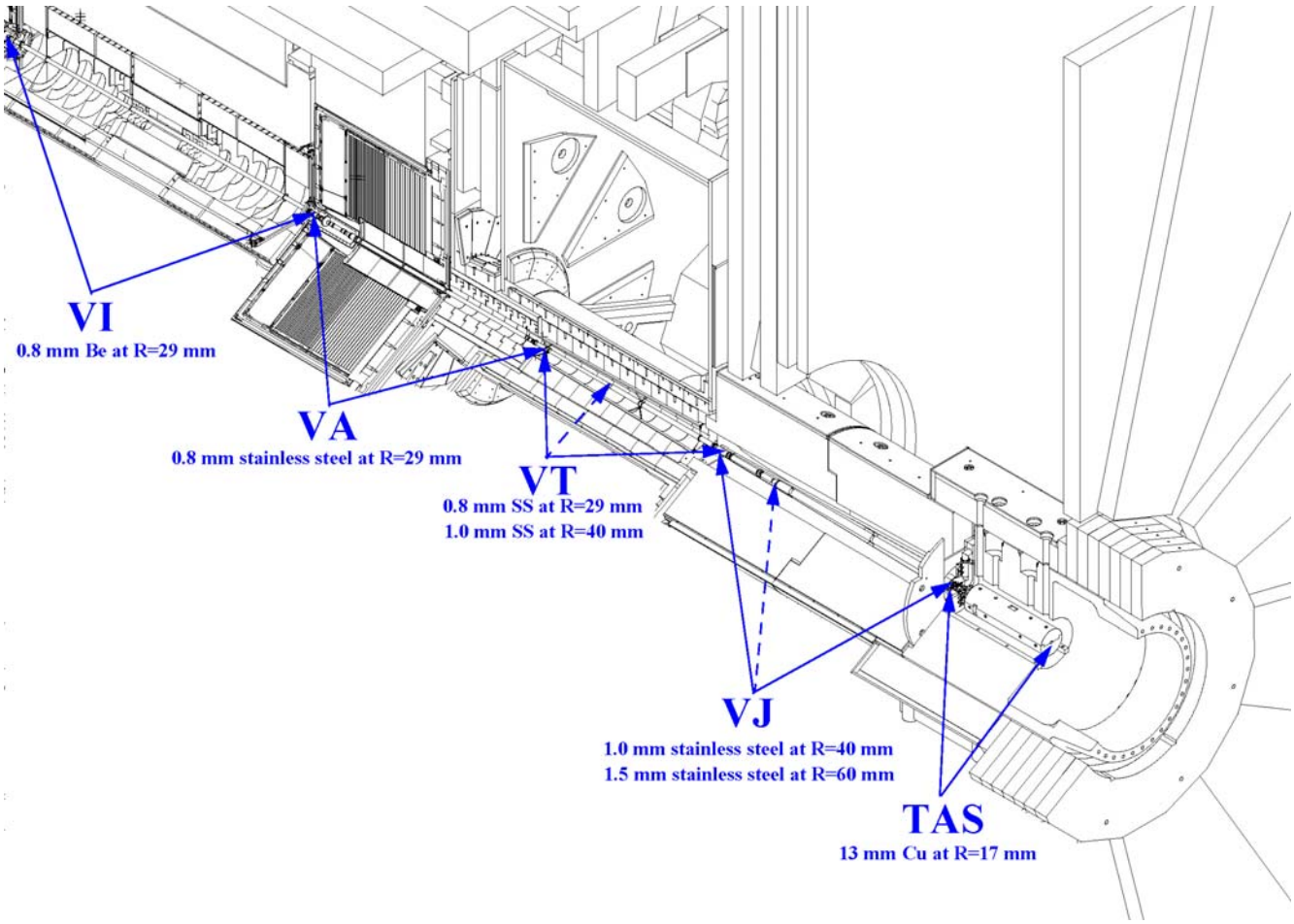

Figure 10. The five beampipe sections in ATLAS. Note that the VT and VJ beampipes have a front section (indicated by a dashed arrow) with a smaller radius than the rest.

Figure 11 show that the removal of the beampipe in the simulation reduces the rates by a factor 2 in the small wheel and the EO chambers (called the "Back wheel" in this note) and by a factor 3 in the barrel and Large wheel. Earlier studies have shown that changing the beampipe material to aluminium would reduce the rates but not by a large factor. A new study has therefore been made in which the beampipe material is changed to beryllium in a region which starts in front of the FCAL and ends in the middle of the forward shielding (z = 4.5-16 m). The results of the simulation are given in Figure 12. A significant reduction of the rates is observed.

If the radius of the beampipe is furthermore increased from 30 mm to 60 mm at the back of the FCAL (z > 6.7 m) then the rates are reduced further and the rates are now close to those without the beampipe (Figure 11). If the beampipe radius were increased in this fashion it would be impossible to retract the endcap calorimeter while leaving the beampipe in place. This would mean that the ATLAS beampipe would have to be removed before any maintenance of the inner detector could be made. It is not clear, however, if this would be a serious drawback of this scenario since not much maintenance of the inner detector can be done with the beampipe in place. Figures 22, 23 and 24 shows contour plots of the photon, neutron and high-energy hadron flux (> 20 MeV). In these figures the plots in position a) show the baseline scenario and b) the situation with a beryllium beampipe (with normal radius). The beryllium beampipe seems to be particularly efficient in reducing the photon background.

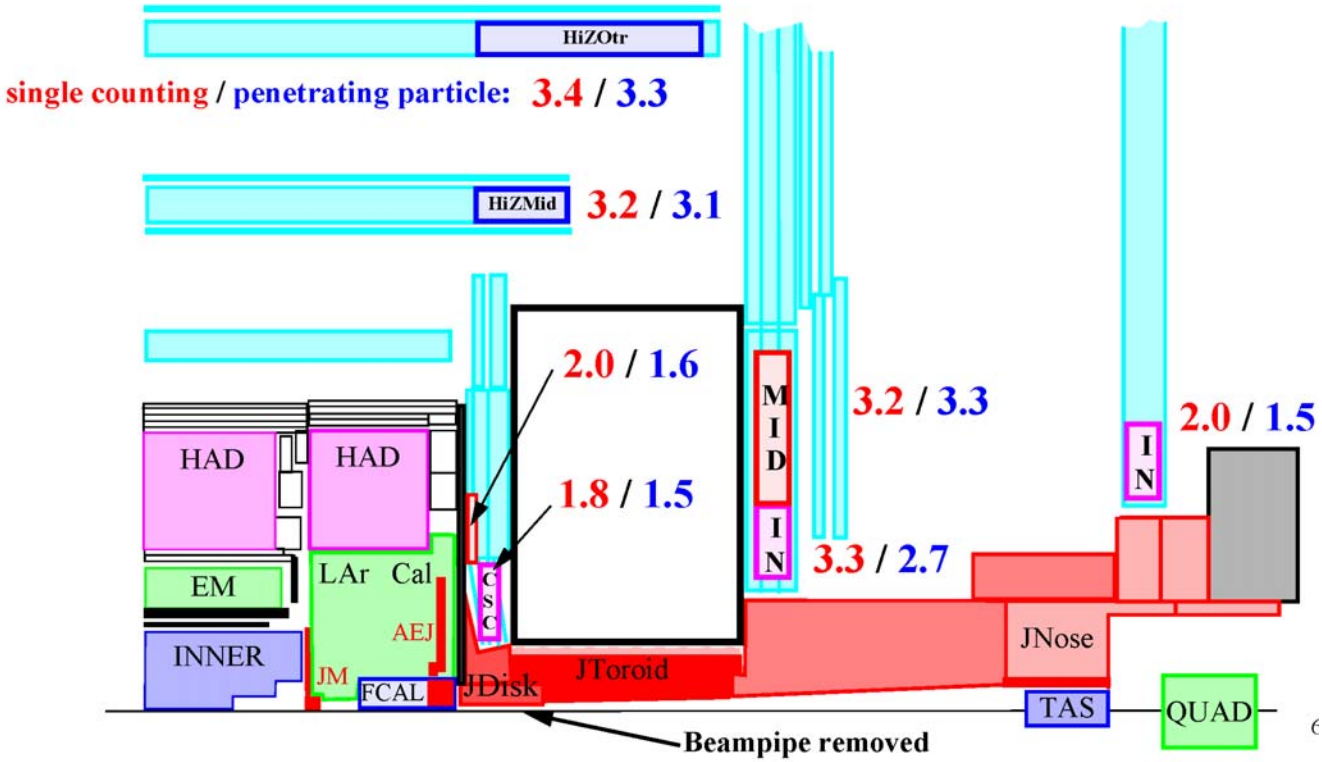

Figure 11. The ratio of muon rates in the present shielding baseline configuration to the rates after the beampipe has been removed in the simulation. Both single muon counting rates and penetrating particles rates are given.

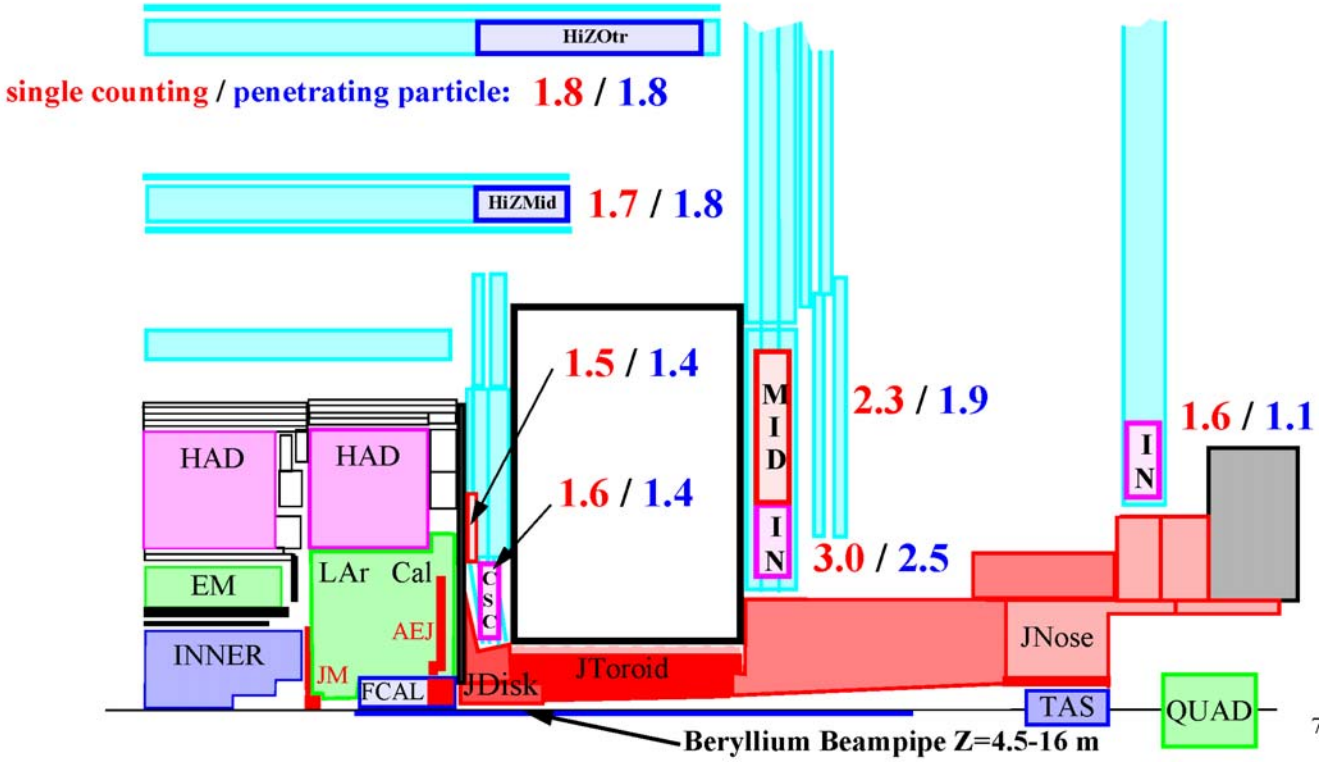

Figure 12. The ratio of muon rates in the present shielding baseline configuration to the rates after the beampipe in z=4.5-16 m has been changed to beryllium. Both single muon counting rates and penetrating particles rates are given.

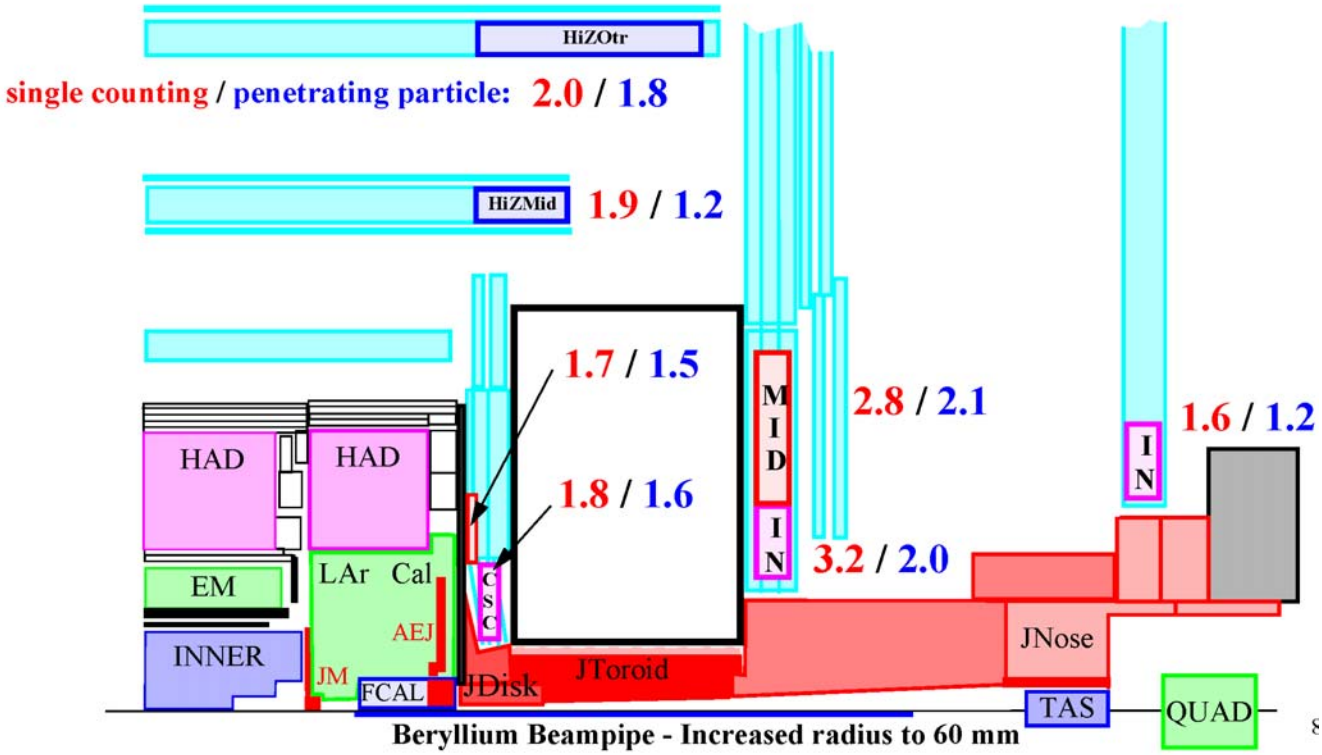

Figure 13. The ratio of muon rates in the present shielding baseline configuration to the rates after the beampipe in z=4.5-16 m has been changed to beryllium and the radius of the beampipe has been increased to 60 mm for z > 7.5 m. Both single muon counting rates and penetrating particles rates are given.

The disk shielding

The region of the muon spectrometer with the largest background rate is the small wheel (see Figure 7). If one is prepared to sacrifice the CSC chambers one could in principle improve the disk shielding by extending the JD hub into the region of the CSC chambers as shown in Figure 14. The present JD hub has an outer radius of 54 cm in the front and 76 cm in the back. This was increased to 150 cm in the simulation while keeping the cladding layers of polyethylene and lead on the outside. This would add another 35 ton of brass to each disk shield which could probably be taken by the present rib and tube construction. The attachment of the new shielding to the hub would, however, not be easy to achieve since the hub has to be able to move on the plug.

The result of the simulation is shown in Figure 15. The background rate is decreased by a factor of two in the small wheel, by 20-30% in the barrel and by nothing in the large and back wheels.

The toroid shielding

Figure 9 shows that there is a large plume of neutron radiation coming out of the endcap toroid. Several simulations have been made to see what would happen if the shielding in the toroid region would be enlarged. In the most extreme of these simulations, a completely new endcap toroid is envisioned with a much larger bore. The radius of the shielding plug in the toroid could then be extended to 150 cm, i.e., 205 tons of brass shielding could be added to each toroid. This would bring the outer radius of the toroid shielding to that of the forward shielding. The polyethylene layer on the outside of the plug would be moved to the new outer radius.

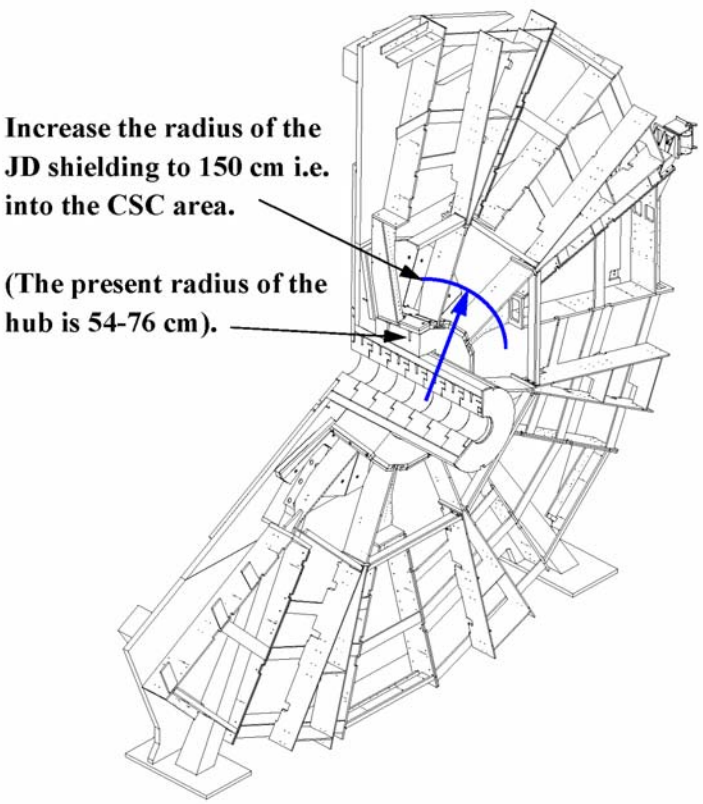

Figure 14. **The disk shielding with the support frame for the detectors in the small muon wheel. An increase of the radius of the hub to 150 cm is indicated by the blue line in the plot.**

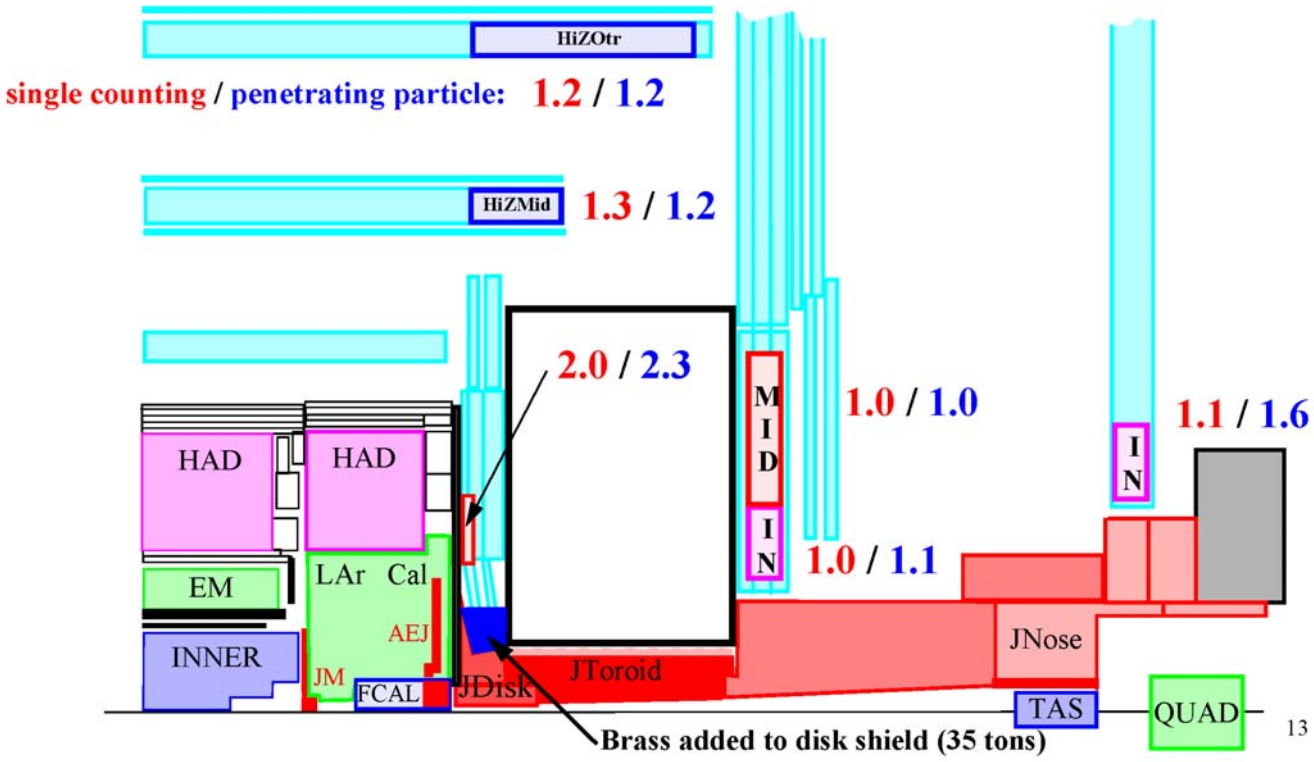

Figure 15. **The ratio of muon rates in the present shielding baseline configuration to the situation after the radius of the JD hub has been increased to 150 cm. Both single muon counting rates and penetrating particles rates are given.**

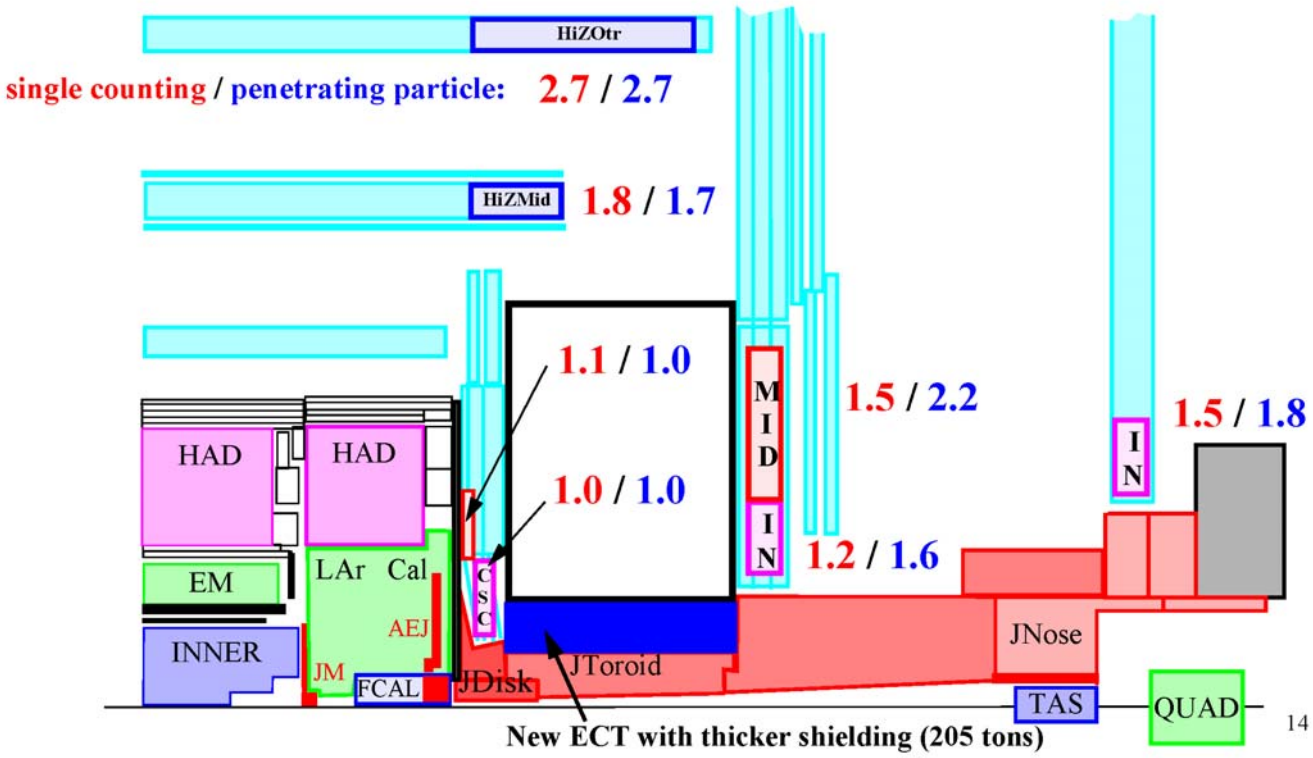

Figure 16. The ratio of muon rates in the present shielding baseline configuration to the situation after the radius of the JT plug in the endcap toroid has been increased to 150 cm. Both single muon counting rates and penetrating particles rates are given.

The result of the simulation is given in Figure 16. There is as expected a large reduction of rate (factor 3) in the barrel detectors that sits in the plume of the radiation coming out from the endcap toroid. There is no reduction, however, in the small wheel and only a modest one in the large and back wheels. Figures 22d, 23d and 24d shows more in detail what happens with the particle flux when the shielding is increased to a radius of 150 cm (starting in the small wheel and going all the way to the back of the forward shielding). The plume of neutron and high-energy hadron radiation is extinguished but the photon flux has not changed as dramatically and this is the reason for the quite modest decrease of the overall rates seen in Figure 16. So even a completely new endcap toroid with reduced acceptance and more shielding would not be able to reduce the background rates by an order of magnitude.

The possibility of changing the JD plug to tungsten from brass has been discussed and studied for years. This would be very costly and only give some 30% reductions in rate. In the present set of simulations this idea has been expanded to include also the plug in the endcap toroid and Figure 17 shows the rates if both the JD and JT plugs are made of tungsten. The reduction in rate in the small wheel for tungsten plugs is comparable to that of the large beryllium beampipe. It is larger in the barrel region that is suffering from the plume and smaller in the large and back wheel region. Tungsten could therefore make a significant difference to the rates. The problem is that some 350 tons of tungsten would be needed and at a price of at least 70 CHF/kg this would cost 25 million CHF.

A less costly approach would be to add brass to the inside of the endcap toroid. Figure 18 shows an old shielding scenario in which some 200 epoxy blocks were placed inside the toroid between the coils. This scenario was discarded for several reasons but mainly because this shielding did not work better than a thin polyethylene layer surrounding the JT plug. These old shielding blocks have now been resurrected in the simulation and turned into brass. The effect is disappointing as can be seen in Figure

19. There is no reduction in rate except in the barrel region of the plume where the rates goes down by 20-30%. This shielding scenario is clearly not worth the effort and cost of implementing it. It can also be noted that with an additional 80 tons of material inside the endcap toroid, the total weight of these magnets would be above the limit of the crane in the SX1 surface building.

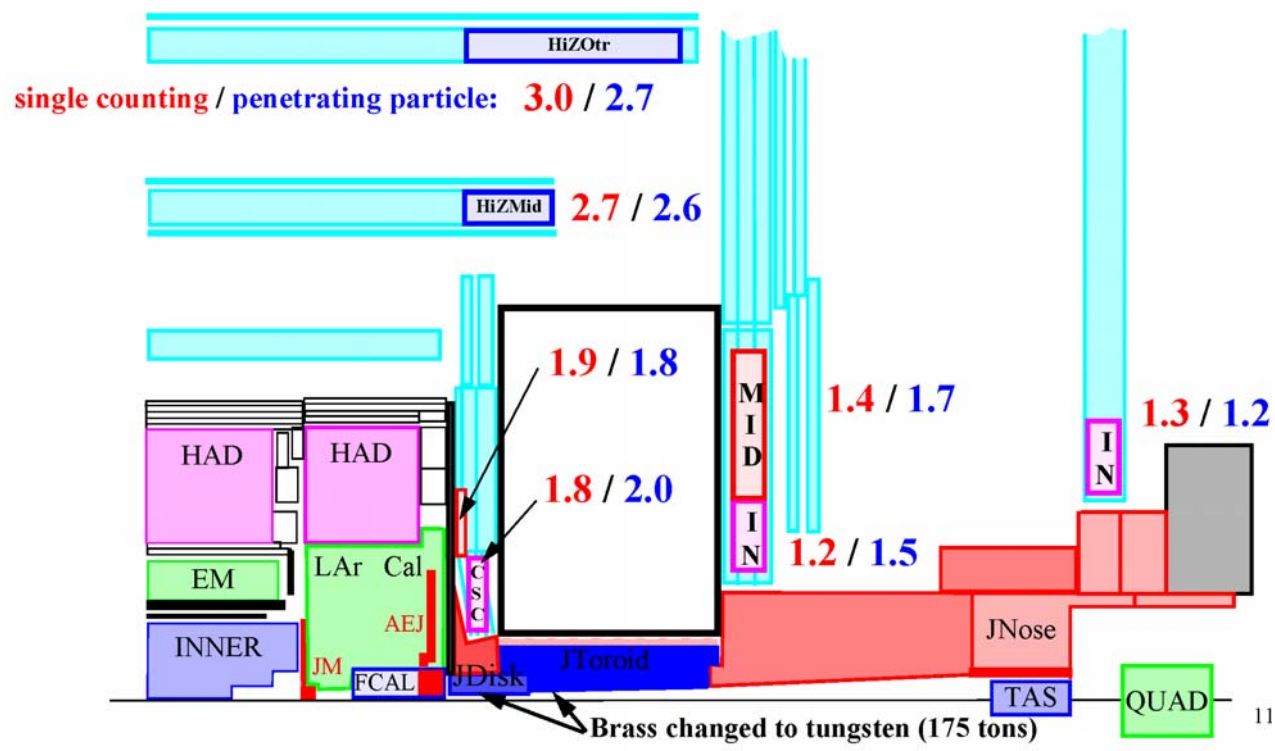

Figure 17. The ratio of muon rates in the present shielding baseline configuration to the situation after the brass in the JD and JT plugs have been turned into tungsten. Both single muon counting rates and penetrating particles rates are given.

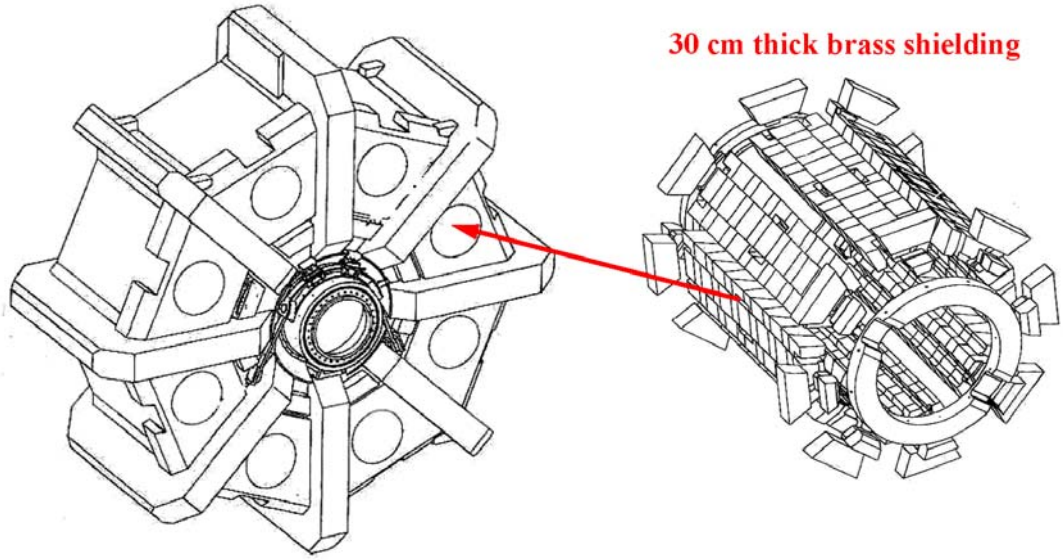

Figure 18. The left plot shows the coils in the endcap toroid. The plot on the right shows the structure of 30 cm thick brass shielding blocks that was introduced between the coils in the simulation.

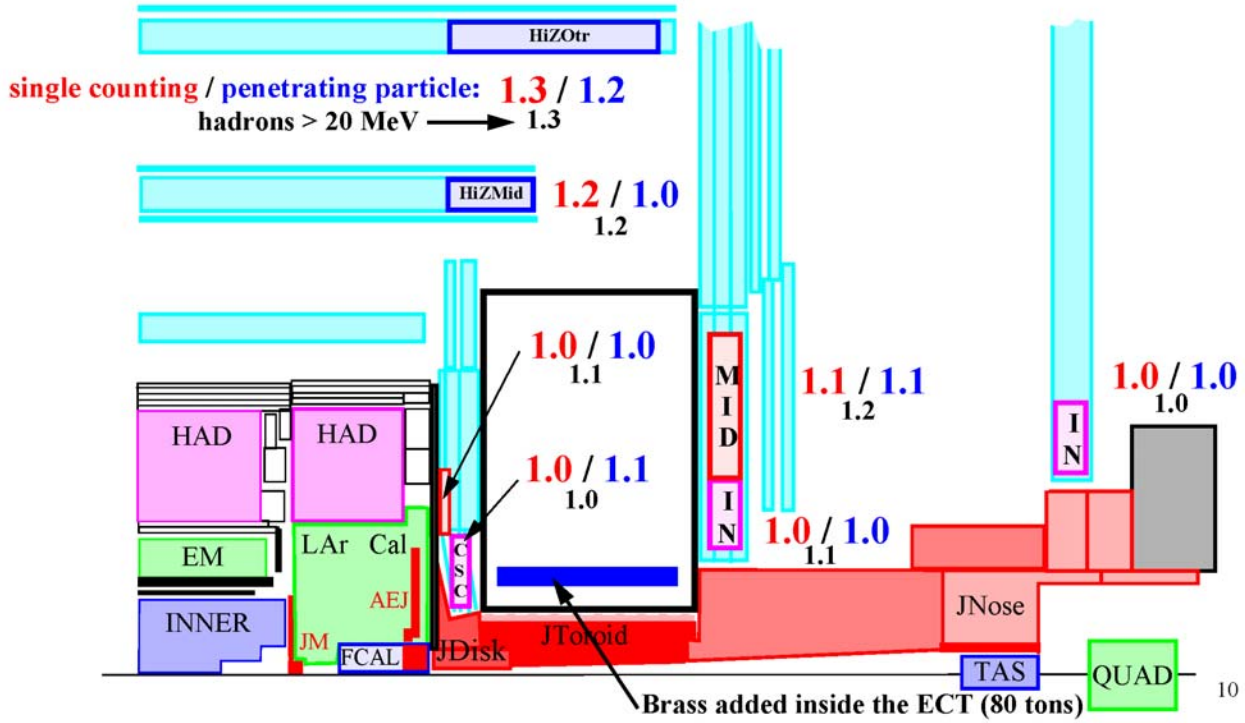

Figure 19. The ratio of muon rates in the present shielding baseline configuration to the situation after brass has been introduced in the endcap toroid. Single muon counting rates and penetrating particles rates are given as well as rates of hadrons with more than 20 MeV of energy.

The forward shielding

The two main sources of background in the region of the forward shielding are the beampipe and the TAS collimator. The TAS collimator is at present surrounded by the large octagonal forward shielding pieces (see Figure 10). These have been designed in such a way as to be easily fitted with an additional layer of 25 cm thick steel plates. This should be sufficient to contain the background from the TAS also at high luminosities and the dominating background in the large wheel is expected to come from the beampipe with some contributions from interactions in the walls of the center hole of the shielding. When the forward shielding was designed it was seen that the radius of the shielding in the region of the large wheel determines the rates to a large extent. When this radius had to be reduced to give way to the support structure of the large wheel, the predicted rates went up and this is the only region for which the predicted baseline rates are significantly higher than in the Muon TDR (see Figure 7). A one meter long steel ring placed in the center hole of the large wheel was therefore introduced in the simulation, as depicted in Figure 20. No cladding was put on the outside of this ring. The radial thickness of the ring was 40 cm and it had a weight of about 37 tons. Obviously this type of shielding ring would require a radical re-design of the large wheel and it is not clear how the ring would be supported.

Figure 21 shows the predicted rates from a simulation with the steel ring in the forward shielding together with a beryllium beampipe (with the present baseline radius) and a larger hub in the JD shielding. This plot should be compared to Figure 12 which shows the change of rate when only the beryllium beampipe is introduced. Clearly the change of the JD hub improves the situation while the improvement due to the steel ring around the JF is not as significant. Figures 22c, 23c and 24c show that while the steel ring reduces the flux of high-energy hadrons, it does not do much to the fluxes of photons and neutrons. It is doubtful that the 20% reduction in muon rates due to the steel ring motivates the changes needed to the large wheel.

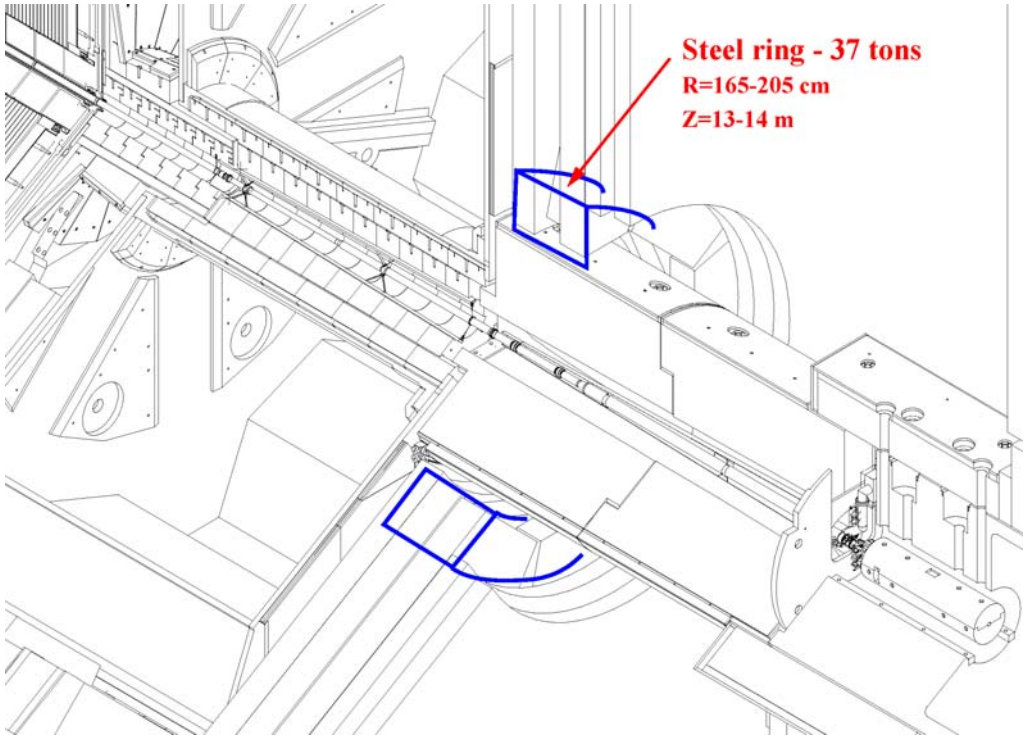

Figure 20. The forward shielding with the large muon wheel surrounding it. An increase of the radius of the forward shielding to 205 cm is indicated by the blue lines in the plot.

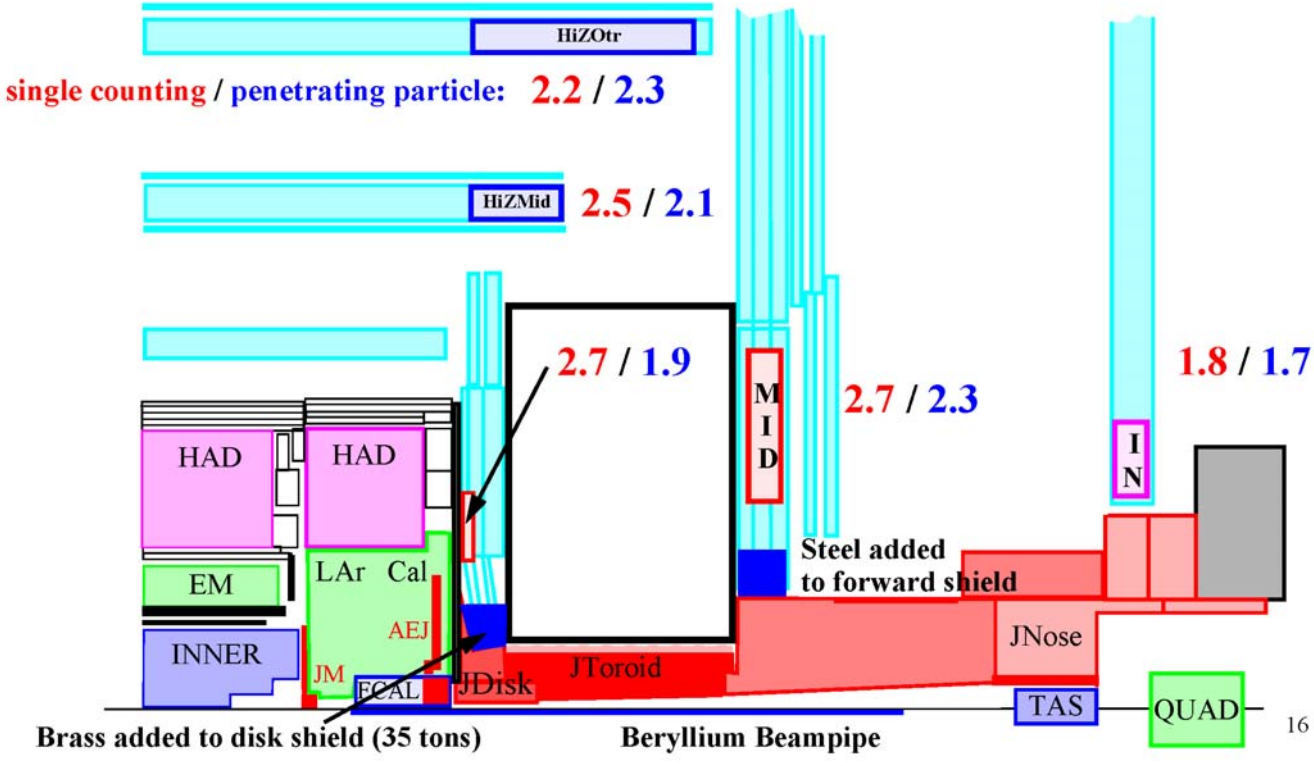

Figure 21. The ratio of muon rates in the present shielding baseline configuration to the situation after the beampipe material has been changed to beryllium and the radius of the JD and JF have been increased. Both single muon counting rates and penetrating particles rates are given.

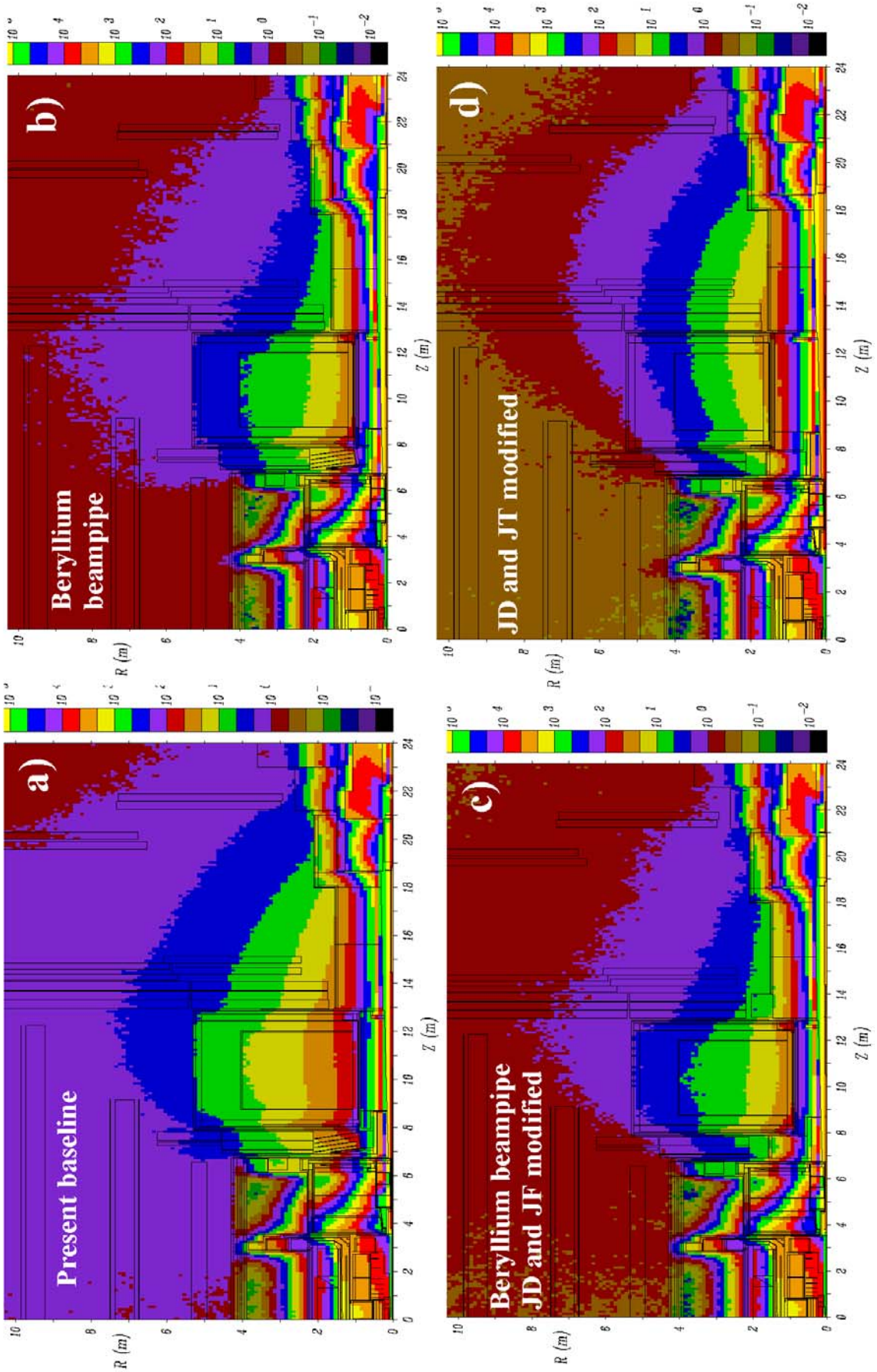

Figure 22. The photon flux in kHz/cm^2 for four different shielding scenarios.

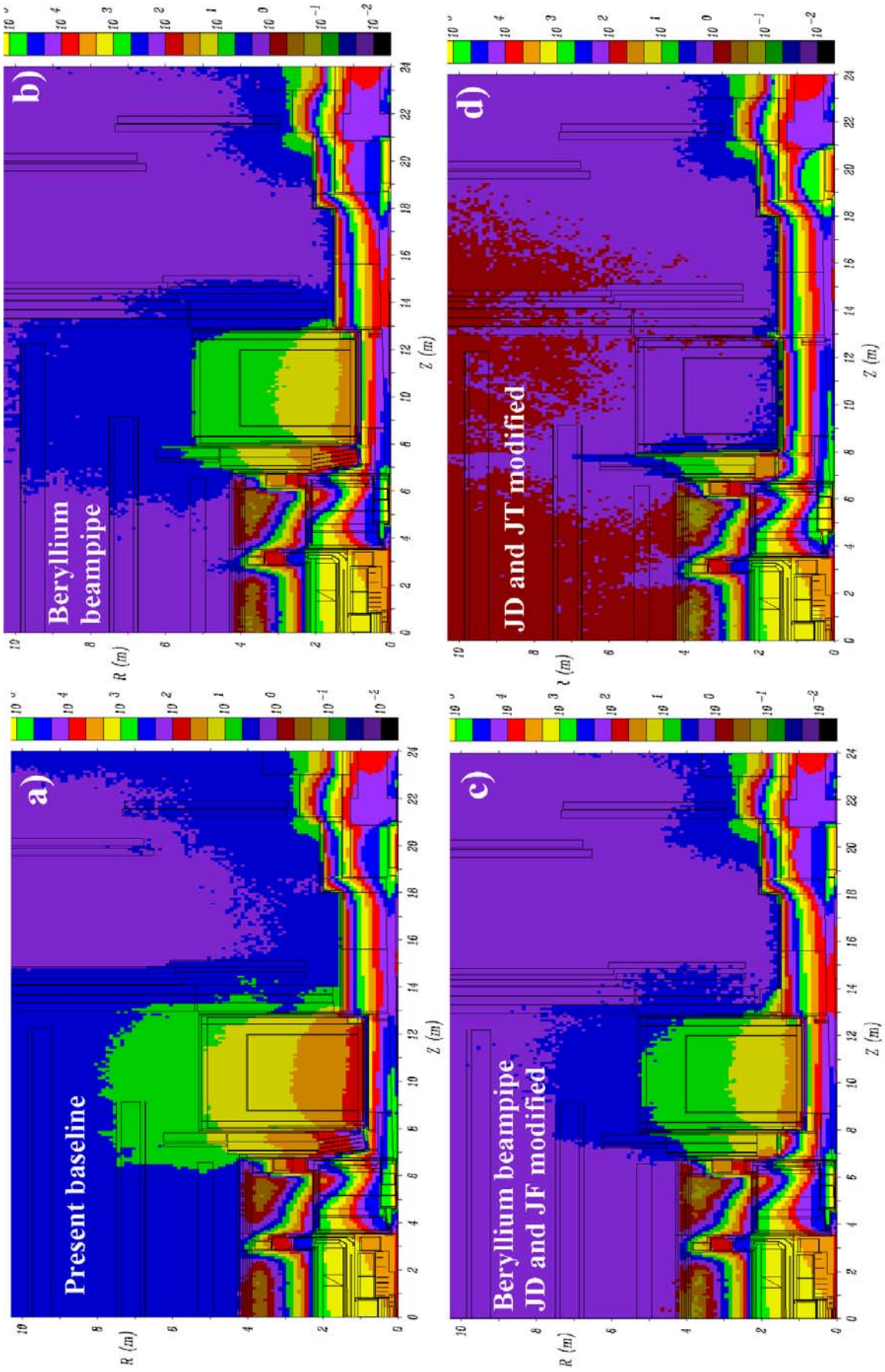

Figure 23. The neutron flux in kHz/cm^2 for four different shielding scenarios.

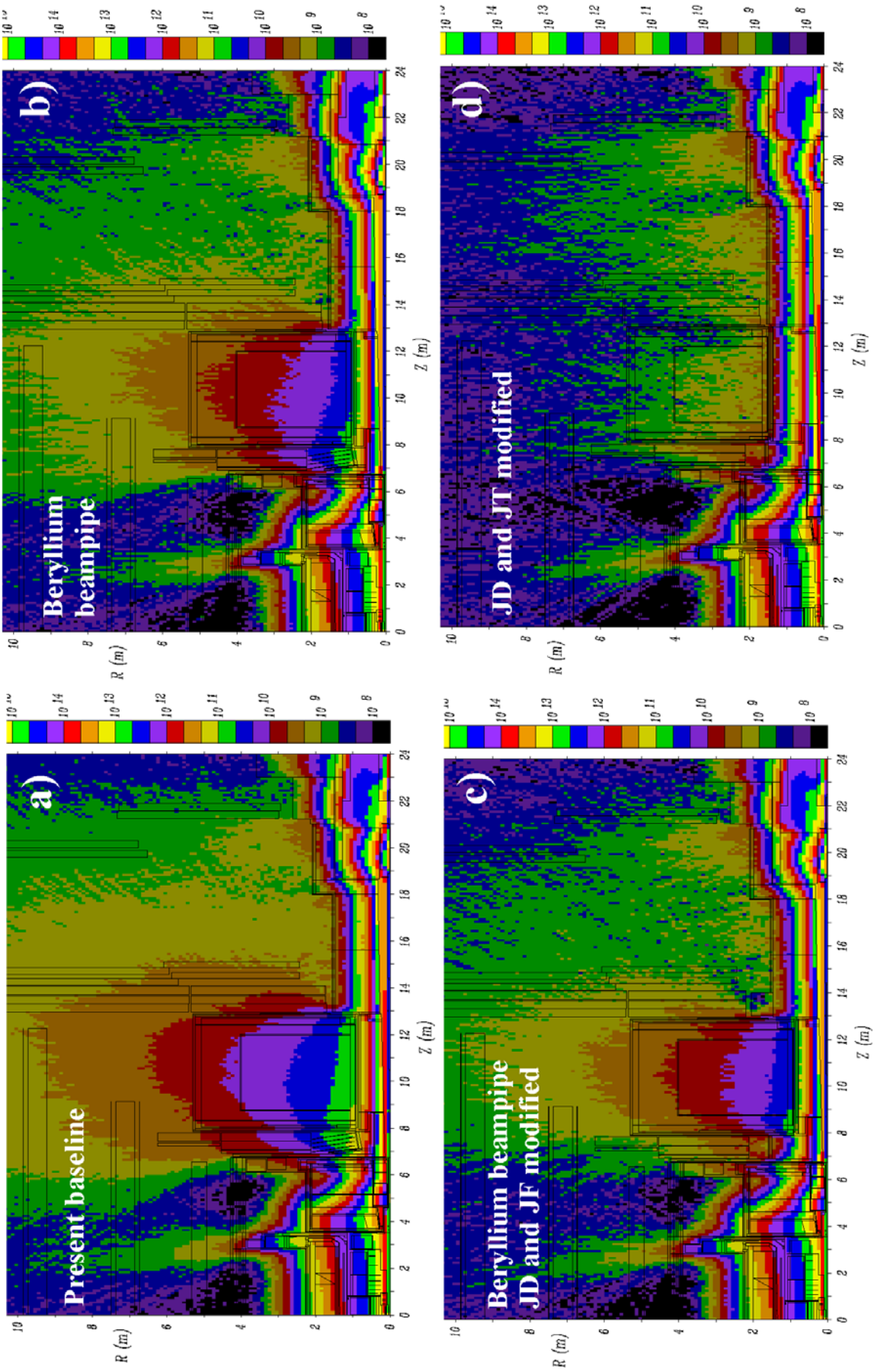

Figure 24. The flux in Hz/cm^2 of hadrons with E>20 MeV for four different shielding scenarios.

5 Conclusions

An increase of the luminosity at the LHC from 10^{34} cm^{-2} s^{-1} to 10^{35} cm^{-2} s^{-1} would mean that the USA15 cavern could not any longer be classified as a simple controlled area. It is also possible that the SX1 surface building would no longer be classified as a supervised area.

Induced activation will be a large problem for ATLAS already at 10^{34} cm^{-2} s^{-1} and at higher luminosities the collaboration should consider changing the beampipe material to beryllium.

A change to a beryllium beampipe would also significantly lower the background rates in the muon spectrometer. The present shielding layout has on the other hand been optimised for years and there is no simple improvement of the shielding that would give a large reduction in background rate. Even drastic and very costly changes to the shielding will not reduce the rates by more than a factor of 3.

The results of the simulations in this note have an uncertainty corresponding to a factor 2-3 in rates and it is therefore important to wait for the first data before any decisions are made about upgrade scenarios.

References

[1] *Protection against ionizing radiation. CERN Radiation Safety Manual.*
http://edms.cern.ch/file/335729/LAST_RELEASED/F_E.pdf

[2] *Radiation in the USA15 cavern in ATLAS,*
I. Dawson and V. Hedberg, **ATL-TECH-2004-001.**

[3] *The ATLAS activation studies.*
http://atlasinfo.cern.ch/Atlas/TCOORD/Activities/CommonSys/Shielding/Activation/activation.html

[4] *Activation study of the ATLAS detector,* V.A. Klimanov, E.I. Kulakova, M.N. Morev and V.K. Sakharov, ISTC Project #1800, April-June 2001, Moscow Engineering Physics Institute.
http://atlasinfo.cern.ch/Atlas/TCOORD/Activities/CommonSys/Shielding/Activation/report_1_2_new.pdf

[5] *Activation dose rate in access scenarios to the area between the disk shield and the toroid,*
V.A. Klimanov, E.I. Kulakova, M.N. Morev and V.K. Sakharov, ISTC Project #1800, July-September 2001, Moscow Engineering Physics Institute.
http://atlasinfo.cern.ch/Atlas/TCOORD/Activities/CommonSys/Shielding/Activation/text_tab_1_4.pdf

[6] *Hadronic photon-photon interactions at high-energies,*
R. Engel and J. Ranft, Phys. Rev. D54 (1996) 4244.

[7] *The GCALOR simulation package,* C. Zeitnitz.
http://www.physik.uni-mainz.de/zeitnitz/gcalor/gcalor.html

[8] *Approximation of Radionuclide Production Cross section in Proton Induced Nuclear Reactions,*
V.G. Semenov and N.M. Sobolevsky, Report in the ISTC project #187, Moscow, 1998.

[9] *The DOT-III Two-Dimensional Discrete Ordinates Transport Code,*
F. Mynat et al., ORNL-TM-4280, Oak Ridge, 1973.

[10] *MCNP - A general Monte Carlo N-Particle Transport Code, Version 4A,*
J.F. Briesmeister, Los Alamos National Laboratory Report, LA-12625, 1995.

[11] *Dose rates between the JT and JN*,
M.N. Morev, ISTC Project #1800, Moscow Engineering Physics Institute.
http://atlasinfo.cern.ch/Atlas/TCOORD/Activities/CommonSys/Shielding/Activation/nose_fields.pdf

[12] *Doses with the LAr (VA) beampipe made in 1.5 mm thick aluminium*,
M.N. Morev, ISTC Project #1800, Moscow Engineering Physics Institute.
http://atlasinfo.cern.ch/Atlas/TCOORD/Activities/CommonSys/Shielding/Activation/va_beampipe_15_real_al.pdf

[13] *Doses from the ID (VI) beampipe*, V.A. Klimanov, E.I. Kulakova, M.N. Morev and V.K. Sakharov, ISTC Project #1800, Moscow Engineering Physics Institute.
http://atlasinfo.cern.ch/Atlas/TCOORD/Activities/CommonSys/Shielding/Activation/vi_beampipe.pdf

[14] *ATLAS radiation background task force summary document*,
M. Bosman, I. Dawson, V. Hedberg and M. Shupe,
http://atlas.web.cern.ch/Atlas/GROUPS/PHYSICS/RADIATION/RadiationTF_document.html

[15] *Electron-photon transport in FLUKA: Status*, A. Fasso, A. Ferrari and P.R. Sala, and *FLUKA: Status and Prospective for hadronic applications*, A. Fasso, A. Ferrari, J. Ranft and P.R. Sala, Proc. MonteCarlo 2000 Conference, Lisbon, October 2000, Springer-Verlag Berlin 2001,
http://pcfluka.mi.infn.it/heart/rh.html

[16] ATLAS Muon Spectrometer Technical Design Report, CERN/LHCC/97-22.
http://atlas.web.cern.ch/Atlas/GROUPS/MUON/TDR/Web/TDR_chapters.html